

ADA082347

Report <sup>15</sup> N00014-78-C-0289

LEVEL <sup>11</sup>

(2)  
5

(6)

REMOTE ATMOSPHERIC WIND SPEED MEASUREMENTS BY INDIVIDUAL PARTICLE  
SCATTERING AND DIGITAL BURST CORRELATION

(10)

C. Y. / She ~~and~~ Richard F. / Kelley  
Physics Department  
Colorado State University  
Fort Collins, CO 80523

DTIC  
ELECTE  
MAR 24 1980  
S D C

(11)

(12)  
7451

Dec ~~1978~~ 1979

Final Report, for Period 1 March 1978 — 31 October 1979

Prepared for

OFFICE OF NAVAL RESEARCH  
800 N. Quincy Street  
Arlington, VA 22217

NAVAL RESEARCH LABORATORY  
4555 Overlook Ave., S.W.  
Washington, DC 20375

This document has been approved  
for public release and sale; its  
distribution is unlimited.

79-12 27 046

FILE COPY

Unclassified

SECURITY CLASSIFICATION OF THIS PAGE (When Data Entered)

REPORT DOCUMENTATION PAGE		READ INSTRUCTIONS BEFORE COMPLETING FORM
1. REPORT NUMBER N00014-78-C-0289	2. GOVT ACCESSION NO.	3. RECIPIENT'S CATALOG NUMBER
4. TITLE (and Subtitle) REMOTE ATMOSPHERIC WIND SPEED MEASUREMENTS BY INDIVIDUAL PARTICLE SCATTERING AND DIGITAL BURST CORRELATION		5. TYPE OF REPORT & PERIOD COVERED Final, 3/1/78 - 10/31/79
		6. PERFORMING ORG. REPORT NUMBER
7. AUTHOR(s) C. Y. She and Richard F. Kelley		8. CONTRACT OR GRANT NUMBER(s) N00014-78-C-0289 <i>new</i>
9. PERFORMING ORGANIZATION NAME AND ADDRESS Department of Physics Colorado State University Fort Collins, CO 80523		10. PROGRAM ELEMENT, PROJECT, TASK AREA & WORK UNIT NUMBERS
11. CONTROLLING OFFICE NAME AND ADDRESS Procuring Contracting Office Office of Naval Research Arlington, VA 22217		12. REPORT DATE December 1979
		13. NUMBER OF PAGES 34
14. MONITORING AGENCY NAME & ADDRESS (if different from Controlling Office) Optical Radiation Branch Naval Research Laboratory Washington, DC 20375		15. SECURITY CLASS. (of this Report) Unclassified
		16. DECLASSIFICATION/DOWNGRADING SCHEDULE
16. DISTRIBUTION STATEMENT (of this Report) Scientific Officer DDC, Code S4 ONR Branch Office ACO NRL, Code 2627 ONR, Code 1021P		
17. DISTRIBUTION STATEMENT (of the abstract entered in Block 20, if different from Report)		
18. SUPPLEMENTARY NOTES		
19. KEY WORDS (Continue on reverse side if necessary and identify by block number) Remote sensing Atmospheric wind measurements Individual particle scattering Photon correlation of digital bursts		
20. ABSTRACT (Continue on reverse side if necessary and identify by block number) We have demonstrated that atmospheric wind speeds can indeed be measured with photon bursts scattered from single dust particles. If photon counting electronics and clipped digital correlation are used for signal analysis, an unambiguous speed measurement can be made with a detected signal as low as ten counts under practical conditions, i.e., in the presence of noise. A microprocessor is used to run the LTV measurements automatically, and to analyze and compare data for both LTV and a conventional cup anemometer.		

This document has been approved  
for public release and sale; its  
distribution is unlimited.

DD FORM 1 JAN 73 1473

EDITION OF 1 NOV 65 IS OBSOLETE  
S/N 0102-014-6601

SECURITY CLASSIFICATION OF THIS PAGE (When Data Entered)

Satisfactory agreement between the LTV and the cup anemometer were obtained. The potential of the LTV with its high speed data acquisition and its short measurement time has been thoroughly demonstrated. In the field test of this automated LTV system, we have conducted speed measurements with both natural aerosols and with seeding of water droplets from a humidifier. To our satisfaction, we obtained better performance without seeding.

In short, with the research of this project, we have demonstrated beyond doubt the principle of single-particle scattering for remote speed measurements and also the practical uses of LTV under realistic field conditions.

Accession For	
NTIS OR&I	<input checked="checked" type="checkbox"/>
DDC TAB	<input type="checkbox"/>
Unannounced	<input type="checkbox"/>
Justification	<input type="checkbox"/>
By <i>Per</i>	
Distribution /	
Availability	
Dist	Approved
<i>A</i>	

REMOTE ATMOSPHERIC WIND SPEED MEASUREMENTS BY  
INDIVIDUAL PARTICLE SCATTERING AND DIGITAL BURST CORRELATION

C. Y. She and Richard F. Kelley

Department of Physics  
Colorado State University  
Fort Collins, CO 80523

Summary

We have demonstrated that atmospheric wind speeds can indeed be measured with photon bursts scattered from single dust particles. If photon counting electronics and clipped digital correlation are used for signal analysis, an unambiguous speed measurement can be made with a detected signal as low as ten counts under practical conditions, i.e., in the presence of noise.

A microprocessor is used to run the LTV measurements automatically, and to analyze and compare data from both LTV and a conventional cup anemometer. Satisfactory agreement between the LTV and the cup anemometer were obtained. The potential of the LTV with its high speed data acquisition and its short measurement time has been thoroughly demonstrated. In the field test of this automated LTV system, we have conducted speed measurements with both natural aerosols and with seeding of water droplets from a humidifier. To our satisfaction, we obtained better performance without seeding.

In short, with the research of this project, we have demonstrated beyond doubt the principle of single-particle scattering for remote speed measurements and also the practical uses of LTV under realistic field conditions.

## Table of Contents

	<u>Page</u>
Report Documentation Page.....	1
Summary.....	ii
List of Figures.....	v
List of Tables.....	vi
I. Introduction.....	1
II. Individual Particle Scattering and Detection Sensitivity.....	3
Total signal counts.....	4
Minimal detectable signal level.....	5
Probability distribution of signal particles.....	8
III. Automated LTV Measurements and Field Tests.....	10
Automatic data acquisition.....	10
Experimental arrangement.....	11
Field tests: Data/system evaluation.....	16
IV. A Method for Measuring Atmospheric Turbulence.....	24
V. Conclusions.....	27
References.....	28
Figures.....	29
Appendix.....	A1

### List of Figures

- Figure 1. Three selected correlation functions resulting from natural aerosol indoors.
- Figure 2. Probability density of burst counts from a uniformly illuminated target.
- Figure 3. Probability density of burst counts resulting from indoor aerosol.
- Figure 4. Experimental arrangement for LTV field measurement.
- Figure 5. Typical correlation functions for seeded aerosol and fan generated wind.
- Figure 6. Typical correlation functions for nature aerosol and natural wind.

### List of Tables

- Table 1. Three selected correlation functions of LTV measurements.
- Table 2. Comparison of cup anemometer velocity and average LTV correlator velocity for natural particles and fan generated wind.
- Table 3. Comparison of cup anemometer velocity and average LTV correlator velocity for seeded aerosol and fan generated wind.
- Table 4. Comparison of cup anemometer velocity and average LTV correlator velocity for natural aerosol and natural wind.



## I. Introduction

Preliminary investigations of wind speed measurements at Colorado State University using a crossed dual beam laser Doppler velocimeter<sup>1</sup> (LDV) and a new parallel dual beam laser time-of-flight velocimeter<sup>2</sup> (LTV), both in a single-ended arrangement, have yielded encouraging results. Field measurements of wind speed under natural aerosol conditions up to a range of 60 m with 0.35 W laser power using a LDV and to a range of 100 m with 0.20 W laser power using a LTV, have been successfully carried out at night. The velocity signal, under either arrangement, is analyzed by a clipped digital correlator. A simple method for measuring the overall aerosol concentration using the same apparatus has been initiated and an expression for the signal arrival rate, which is, in our opinion, a useful figure of merit for these types of velocimeters, has been derived.<sup>3</sup>

The fact that it is possible to make an unambiguous velocity measurement with photon bursts scattered from a single dust particle is by no means widely recognized. The concept of single particle scattering and burst correlation is further studied and substantiated in this report, both theoretically and experimentally.

With the concept of individual particle scattering firmly established, the feasibility of practical applications using single-particle correlation for remote wind speed measurements is demonstrated. A microprocessor is used to control and operate the experiment. Data from the single-particle correlation for wind speed determination and that from a cup anemometer are analyzed by the microprocessor in real-time. The operation of this automated system both in the laboratory and

in the field is described. Preliminary performance has been quite satisfactory.

Attempts to measure the effect of atmospheric turbulence on the propagation of focussed laser beams is also described in this report. A method using a diode array to probe turbulence effect in a short time scale (on the order of milliseconds) is suggested.

The organization of this report is as follows. The concept of single-particle scattering and the method of burst correlation are described in Section II. About half of the significant results in this section have already been published<sup>4</sup> for which a reprint of the published article is included in the Appendix without further explanation. Only new data and interpretations of single-particle scattering and their associated photon bursts are described in the main text of this report. The automated operation and data acquisition along with the tests of its operation in the field are described in Section III. A brief discussion on a new concept for probing atmospheric turbulence is given in Section IV. Section V summarizes the research achievements carried out in the duration of this project.

## II. Individual Particle Scattering and Detection Sensitivity

Both laser techniques (LDV and LTV) for wind speed measurements make use of two laser beams which set up a predetermined spatial pattern in the region of interest. This pattern consists of a set of parallel interference fringes in the case of LDV and it simply consists of two intense spots in the case of LTV. As a particle traverses across this region of interest, an image of the pattern is recorded in real-time. The speed of the traversing particle is then measured by the ratio (of the scale) of this pattern in space to its recorded image in time.

It should be obvious that the visibility of the recorded image pattern (in time) plays an important part in the signal-to-noise of a measurement. When many randomly spaced particles traverse the viewing volume together (even with the same velocity), the visibility of the detected image pattern is very much reduced as compared to that of the original pattern set up by the laser beams in space. For this reason, a speed measurement should be made with light scattering from a single dust particle if it is at all possible. This somewhat surprising stipulation, which is not yet widely appreciated, suggests that a sensitive technique is required to detect weak photon bursts scattered from a single dust particle and that seeding may even produce adverse effects in atmospheric wind measurements.

In the published article (in Appendix), theory of single-particle scattering was compared to that of multiple-particle scattering. The visibility of the detected image patterns due to single-particle scattering and multiple-particle scattering has been investigated and the results substantiated our expectations. By using various preset time intervals for speed measurements and monitoring the corresponding

frequency of successes, it was established that the signal is indeed the result of single particles and that the time for obtaining a single-burst correlation is very small, typically a few milliseconds.

In terms of detection sensitivity, it was estimated that a 2  $\mu\text{m}$ -diameter dust particle scattered from a 0.1 W laser beam at a distance of 20 m away, could, during its transit, yield 200 detected photon counts.<sup>4</sup> The fact that this is enough for a speed measurement is evident because Fig. 7 of the published article<sup>4</sup> shows correlation functions with total signal photon counts ranging from 40 to 800. However, the question of minimal detectable signal level was not discussed. The availability of signal particles in the atmosphere, each of which can scatter enough photons for an unambiguous speed measurement, and the manner in which the detection process discriminates against smaller particles, which are too many to be useful for single-particle scattering, have not been elaborated. These points will now be discussed. Instead of using LDV data operated manually as in the published article, automated LTV data from experiments in the laboratory will be used to support the discussion.

#### Total signal counts

The correlation function of the scattered photon bursts,  $R(\tau)$ , when analyzed, gives not just the speed of the traversing particle. The measured single-clip correlation counts for  $\tau = 0$  actually gives the total counts (at least approximately) of the detected photon bursts due to an individual particle. To see this, we recall that the digital correlation function of the detected photon bursts may be expressed as

$$R(\tau) = R(j\Delta\tau) = \frac{1}{N} \sum_{i=1}^N n(i)n(i-j)$$

where  $n(i)$  is the number of photons in the  $i$ -th interval and  $\Delta\tau$  is the time per correlation channel.  $N$  is the total number of samples used to evaluate the correlation function. For single-clipped correlation,<sup>5</sup>  $n(i) = 1$  if it exceeds a preset level, and  $n(i) = 0$  otherwise. During the presence of the photon bursts scattered from a signal particle, we expect the photon counts  $n(i-j)$  to exceed the preset clipping level. In the absence of noise, the clipped correlation at  $\tau = 0$ , or  $j = 0$  would be, at least approximately,

$$R(0) = \sum_{i=1}^N n(i)$$

which is just the total number of signal counts. Therefore, the counts of the detected photon bursts, equal to  $R(0)$  minus the noise background, can be read directly from the correlation function at  $\tau = 0$ .

#### Minimal detectable signal level

In order to answer this question of minimal detectable signal, many LTV speed measurements under identical conditions (except for the uniformity of aerosol sizes which can not be controlled or pre-determined prior to an experiment) were made in the laboratory. The LTV experiment was set up in a small room and baffles were used to minimize the stray light. The experimental parameters were:  $P$  = laser power in the sensing volume = 85 mW,  $\Delta\Omega$  = detection solid angle  $\approx 10^{-5}$  sr, and  $r$  = range  $\approx 1$  m. The flow was produced by a fan which gives a speed of approximately 4.5 m/sec in the sensing volume. The beam diameter was 1 mm and beam separation 2 mm. The clipping level was set at clip 1 and the sample time used was 20  $\mu$ sec/channel. The measurement time was preset at 2 sec. or  $10^5$  samples.

Three selected correlation functions are shown in Fig. 1. Figure 1(a) corresponds to a particle just big enough for a speed measurement. Although the signal-to-noise is not great, two humps are clearly discernable. The total signal counts is seen to be less than 10 counts. Figure 1(b) represents background noise which has been somewhat reduced by the preset clipping level. And Fig. 1(c) depicts a beautiful correlation function from which particle speed can be determined accurately. Even for this high level of signal-to-noise, only 150 signal counts are needed. The data for the correlation functions in Fig. 1 are also tabulated. This is given in Table 1. There are four numbers in the first row; they give respectively the total photon counts of the experiment (signal counts plus noise counts), clipped counts, 0, and total number of samples for the experiment. The remaining 48 numbers are the correlation counts for 1 to 48 delay channels. Notice the total signal plus noise counts are nearly the same for all three cases while the total signal counts are quite different. This suggests that the single-particle signal bursts occur during a very short time, about  $4 \times 10^{-4}$  sec. in these cases. The clipped count, on the other hand, gives a fairly good idea of the signal bursts.

In the absence of noise, a photon burst of two counts, one scattered from each beam, is in principle enough for a speed measurement. However, even with clipping, some noise is present; ten signal counts is seen to be enough for a speed measurement in practice. The sensitivity of burst correlation is clearly demonstrated. As a side point, we point out that the second peak in Fig. 1(c) is seen to be taller than half of the first peak. Some reflection will show that this is due to the distortion caused by the process of clipping. Although the shape of the

Table 1. Three Selected Correlation Functions of LTV Measurements

Channel Marker	Correlation Counts									
	1308	14	0	100000						
01	7	6	3	0	0	0	0	0	0	0
11	0	0	0	0	0	0	1	1	1	3
21	4	4	4	2	1	0	1	0	0	0
31	0	1	0	1	0	0	0	1	1	1
41	1	0	0	1	0	0	1	0		
	1366	10	0	100000						
01	1	1	1	0	1	0	0	0	1	0
11	0	0	0	0	0	0	0	0	0	0
21	0	0	0	0	0	0	0	0	1	0
31	0	0	0	0	0	0	0	1	0	0
41	0	0	0	0	0	0	0	0		
	1544	33	0	100000						
01	145	133	102	76	48	32	13	7	5	2
11	4	4	11	23	47	66	85	95	102	104
21	103	102	94	82	58	40	22	10	3	1
31	0	1	0	0	0	0	0	0	0	0
41	0	0	0	0	0	1	0	0		

correlation function may be distorted this way, neither the separation between two peaks nor the measured speed will be altered by the clipping process.

#### Probability distribution of signal particles

Natural aerosols come in different sizes. To the first approximation, they may be described by a Junge distribution. There are many small particles in the sensing volume at any instant. Together these particles scatter nearly a constant amount of light and give rise to a Poisson distribution in detected photon counts. A small fraction of larger particles (called signal particles) can yield photon bursts depending on their sizes. The distribution of these signal particles (Junge as opposed to Poisson) may be determined from the measured distribution of photo-burst counts. Therefore, the deviation from Poisson distribution in the measured count probability distribution reveals the presence and the nature of signal particles. The basis of this concept for determining the distribution of signal particles has been investigated before<sup>3</sup> and it has been recently applied to the detection of fluorescence bursts from single atoms.<sup>6</sup>

To demonstrate the usefulness of this concept for burst correlation and speed measurements, we measured the probability density of photo-counts in a preset time interval with one laser beam blocked. The time interval is chosen to be long enough to permit the detection of all counts from a single particle when it traverses the sensing volume. For the same flow condition as used in the speed measurements, we set the time interval to be 1 msec. The desired probability distribution can be determined with the same digital correlator operating in the probability



density mode. For convenience, we took  $10^6$  bursts for each measured distribution of photon counts.

For the purpose of comparison, we first measured the count distribution of bursts scattered from a blackened cardboard paper and the result is shown in Fig. 2. Notice, as expected, the outstanding agreement between the measured distribution and the calculated Poisson distribution with the same mean counts/sample  $\bar{n}$ . The count probability distribution for photon bursts from natural aerosol indoors is shown in Fig. 3. The apparent deviation from the calculated Poisson distribution with the same mean counts/sample, is evident. The presence of larger signal particles which yield detected burst counts ranging from 6 to over 50 is clearly shown. It should be pointed out that although the largest burst shown in Fig. 3 registers 47 counts, this is limited by the available channels in our correlator storage memory, not by the lack of even larger particles in the aerosol. The gradual tailing off of the distribution in Fig. 3 indicates the availability of larger particles with very small probability. Although the power in the sensing volume here is somewhat different from the power used for speed measurements resulting in data shown in Fig. 1 (we used 152 mW here rather than 85 mW), the range of the total signal counts is certainly in good agreement in both cases.

### III. Automated LTV Measurements and Field Tests

To demonstrate the practical feasibility of wind speed measurements with a LTV, we assembled an automated system for operation. A microprocessor is used to control the digital correlator and analyze the data from both the correlator and a conventional cup anemometer. The procedure for automatic data acquisition and the results of the field tests both with a seeded flow and under the conditions of natural aerosols and natural flows are reported below.

#### Automatic data acquisition

During the development phase of a program, manual data collection and analysis is acceptable. For ongoing data collection a method must be employed to reduce the amount of time spent in routine data collection and analysis. This may be accomplished by the computer, and today by the microprocessor.

In this project, the data collected from each experimental run of the digital correlator was stored in the microprocessor. This data consisted of total number of counts, total number of clipped counts, zero, total number of samples, and the 48 correlation function data channels. Analysis consisted of determining time-of-flight and speed. The wind speed and direction from the conventional cup anemometer was collected and stored in the microprocessor for comparison to the wind speed measured by the correlator. The microprocessor program input to the microprocessor was accomplished through the paper tape reader on the teletype.

The microprocessor employed in this research is the MCS6502 based JOLT system built by Microcomputer Associates, now part of Synertek. It has a standard 8 bit data bus and 16 bit address bus. The system has

12 K bytes of random access memory (RAM), which is expandable to 64 K bytes, four input-output (I/O) devices, which gives 8 I/O ports, and teletype interfacing via voltage or current loop. The resident control program, DEMON, is stored in read only memory (ROM). An assembler routine is stored in programmable read only memory (PROM).

The hardware interface between the microprocessor and the Malvern K7023 digital correlator is relatively simple, since both are TTL compatible. This allows wiring I/O ports of the microprocessor directly to the control port and calculator (data and status) port of the correlator.

The software interface is not so simple. It should be mentioned that the microprocessor hardware and software are not independent. Full understanding of the microprocessor software should be obtained before attempting hardware interface to the microprocessor.

The software is the microprocessor program made up of machine instructions encoded in a hexadecimal format. In this research, the microprocessor program was written to collect correlator and cup anemometer raw data, analyze the correlator data to obtain the wind speed and print the results in a suitable format. After initially entering the program through the teletype keyboard, the program was written onto paper tape for subsequent entry into the microprocessor via the paper tape reader.

The microprocessor program is composed of the following routines: initialization, data transfer from correlator to microprocessor, data averaging, time-of-flight determination, correlator speed calculation, and printout.

The initialization routine sets up the I/O ports as either input or output, loads working registers (memory locations) with initial values,

resets and starts the cup anemometer, and stops, resets, and starts the correlator.

The data transfer routine waits for the correlator to stop the experimental run. After the correlator is stopped, the routine stops and starts the data readout from the correlator. The routine stores each channel of data into memory, upon receipt of the appropriate ready signal from the correlator.

The data averaging routine takes the average of the data in channels  $X-1$ ,  $X$ ,  $X+1$ , and stores this average in channel  $X$ . The raw data is preserved.

The routine for time-of-flight determination counts the number of channels to the second peak of the correlation function. It accomplishes this by looking for at least five increases in counts from one channel to the next. It then stops when a decrease in counts occurs. After determining the number of channels to the second peak, the routine multiplies this number by the time per channel (sample) to obtain the time-of-flight of the particle(s).

The velocity calculation routine divides the beam separation distance by the time-of-flight to obtain the correlator wind speed. The program continues reading experimental data from the correlator and reads the cup anemometer wind speed and direction for an appropriate number of correlator experimental runs until the number of runs is completed, or until memory is full.

The printout routine transfers to the teletype for printout: number of times zero clip counts, number of times no correlation function, beam separation, time per channel, and the raw data for each run

with the computed speed, as well as cup anemometer wind speed and direction.

The current size of microprocessor memory allows the data from 90 correlator experimental runs to be stored. Many more runs could be accomplished if the raw data were not preserved for print-out, and only computed speed and cup anemometer speed and direction were stored.

At present, the teletype presents a bottleneck because of its slow bit transfer rate. It takes approximately 45 minutes to print 90 experimental runs. However, an advantage of using the microprocessor is that it is not restricted in the I/O devices that can be attached to it. In the future, data might be transferred to magnetic tape for later analysis on a large computer. Also, the microprocessor program may be changed easily to implement other data analysis techniques.

#### Experimental arrangement

The experimental arrangement utilized in the outdoor field measurements is illustrated in Fig. 4. The laser used is a water cooled Spectra Physics Model 165 Argon-Ion laser operated at 5145 Å in light control mode. It is capable of at least 1.5 W power output at this wavelength. The output of the laser is sent to a Malvern Model RF307 Beam Splitter. The total power output of the beam splitter is 72% of the power into it. The power out is split 55%-45% into the two beams.

The two beams from the beam splitter are directed into the eyepiece of the focussing telescope in order to focus the two beams at the sensing volume. The beam separation  $D$  may be measured directly at the sensing volume. It has been found that this method is not satisfactory due to the large error present in measurement of a small distance, and due to scintillation and beam wander. A more satisfactory method is to measure

the interference pattern spacing  $G$  in front of the focussing telescope, and then determine<sup>2</sup>  $D$  from  $D = (R\lambda)/G$ . This may be used, since this setup may be thought of as two beams diverging from the sensing volume to form an interference pattern at the telescope. Then, if  $G$  is measured in front of the telescope, the range  $R$  is the distance from the point of measurement of  $G$  to the point of measurement at the sensing volume. The point of measurement at the sensing volume is determined by placing a vertical target, a piece of cardboard, centered with respect to the fan, in the sensing volume. The fan is used not only as a support for the target, but also as a wind generator when the natural wind is too small.

The target is used also in visual alignment of the light collected by the 8" Celestron Schmidt-Cassegrain Receiving Telescope into the 400- $\mu$ m diameter aperture mounted in the Malvern RF300 shielded housing. The light accepted by the aperture is collected by the ITT FW130 photomultiplier tube (PMT) with S-20 photocathode mounted in the RF300 housing. The received light from the telescope is defocused to a doughnut shape on the front of the aperture. The telescope horizontal and vertical controls are used to position the doughnut of light around the aperture. The tripod horizontal and vertical controls are used to maintain the doughnut shape of the received light. In the vicinity of the aperture, under proper adjustment, both sets of controls have the same positional effect on the light. The light is then focussed into the aperture.

After visual alignment is accomplished, then the electronic alignment is accomplished utilizing the digital ratemeter. The photomultiplier cathode voltage is increased until counts above background register on the ratemeter. The tripod controls, which are finer adjustments than

the telescope control, are then adjusted for maximum count rate on the ratemeter. This process must be done at low laser power because the reflectivity of the cardboard target is quite high. Lack of care in this respect may result in the PMT "burning out". After this adjustment is accomplished, the PMT cathode voltage is reduced to zero, and the cardboard target is removed from the sensing volume.

If the fan is to be used, the conventional cup anemometer is placed in the laser beam, the fan turned on, and the cup anemometer speed recorded. Then, the cup anemometer is moved out of the beam to its experimental position and its speed is recorded again. From these measurements, a scale factor may be computed to obtain sensing volume fan wind speeds with the cup anemometer out of the sensing volume. Either natural aerosols or seeded aerosols may be used. The seeded aerosols are water particles generated by a humidifier or by a spray bottle.

If natural wind and aerosols are to be used, the fan is moved away, but the anemometer vane is oriented so that zero degrees direction coincides with the laser beam's direction.

With the receiving telescope adjusted, the anemometer set up, and the program entered into the microprocessor, the anemometer wind velocity is measured to compute an approximate time per sample to set into the Malvern K7023 digital correlator. With this accomplished, several manual runs are done to observe if any correlations can be observed. If so, the appropriate information is input to the microprocessor and control given to the microprocessor. During the microprocessor runs, the correlation function can be observed on an oscilloscope, and cup anemometer speed and direction observed on the anemometer electronics digital readout.

Field tests: data/system evaluation

The evaluation of the Laser Time-of-Flight Velocimeter (LTV) utilizing photon counting with clipped digital autocorrelation analysis was accomplished by comparing the wind velocity computed from the correlation function to the wind velocity computed from a conventional cup anemometer. This was accomplished indoors utilizing natural room particulates and fan generated wind. In the field (outdoors), three conditions were utilized: natural particulates with fan generated wind, seeded aerosol from a humidifier with fan generated wind, and natural particulates with natural wind.

The system works quite reliably indoors. The agreement and consistency between the measurement of cup anemometer and the LTV is excellent. The quality of measured correlation functions as shown in Fig. 1 is also excellent.

The outdoor measurements of wind velocity were obtained at the Christman Field facility of Colorado State University, using the setup in Fig. 4. This setup has been described previously.

The range  $R$  selected for these measurements was 25 to 27 meters with a separation angle  $\alpha$  of approximately  $17^\circ$ . The laser power measured at the sensing volume ranged from 27 mW to 56 mW. Background light into the photomultiplier tube (PMT) and the dark counts of the tube yielded 4-10 counts/sec. at a PMT cathode voltage of 1600 V, and 35-50 counts/sec. at 1800 V.

The natural aerosol, fan generated wind condition was attempted first. Representative data is presented in Table 2. The atmosphere was relatively calm that night, which is desirable when the fan is used.

The laser power measured at the sensing volume was 52 mW. The beam separation was  $1500 \pm 100 \mu\text{m}$ . The data in Table 2 shows relatively good



Table 2. Comparison of Cup Anemometer Velocity and Average LTV Correlator Velocity for Natural Particles and Fan Generated Wind

Cup Anemometer Velocity (m/s)	Average LTV Correlator Velocity (m/s)	Number of Data Points in LTV Average Velocity
9.0 $\pm$ 0.5	8.64 $\pm$ 0.52	10
8.5 $\pm$ 0.5	8.47 $\pm$ 0.60	23
8.0 $\pm$ 0.5	8.27 $\pm$ 0.38	29
7.5 $\pm$ 0.5	8.70 $\pm$ 0.14	3

agreement between the cup anemometer and the LTV correlator, except for a cup anemometer velocity of  $7.5 \pm 0.5$  m/s where only 3 data points are available.

The error of  $\pm 0.5$  m/s in the cup anemometer velocity is based on a digitizing error of  $\pm 1$  MPH in the cup anemometer electronics. The error in the average LTV correlator velocity from propagation of errors<sup>7</sup> based on error in beam separation was found to be 0.34 m/s which is less than the standard deviations<sup>8</sup> found, except for the slowest velocity of the cup anemometer.

Because of recurring rains and the necessity for several days to a week of dry weather to obtain sufficient natural aerosols, the measurement using seeded aerosol and fan generated wind conditions was attempted next. Representative data is shown in Table 3 and representative correlation functions are shown in Fig. 5.

The laser power measured at the sensing volume was 41 mW. The beam separation was  $1225 \pm 63$   $\mu$ m. The particles were generated by a humidifier directed into the rear opening of the fan.

The data in Table 3 shows relatively poor agreement between the cup anemometer and the LTV correlator. Other experiments run under these same conditions produce the same or worse results. The error in the average LTV correlator velocities is the standard deviation. In all cases the standard deviation is greater than the error introduced by the propagation error based on the error in the beam separation.

Several reasons may be advanced for the disagreement. First, the conventional cup anemometer is designed for a large scale wind blowing on all the cups. In this experiment, the cup anemometer was placed such that the fan-generated wind blew on one cup only at a time,

Table 3. Comparison of Cup Anemometer Velocity and Average LTV Correlator Velocity for Seeded Aerosol and Fan Generated Wind

Cup Anemometer Velocity (m/s)	Average LTV Correlator Velocity (m/s)	Number of Data Points in LTV Average Velocity	Propagation Error
$9.2 \pm 0.5$	$6.76 \pm 0.46$	8	$\pm 0.12$
$8.7 \pm 0.5$	$6.28 \pm 0.35$	9	$\pm 0.11$
$7.6 \pm 0.5$	$5.96 \pm 0.20$	4	$\pm 0.15$

since the area of the fan opening is so small. This would register a larger wind speed by the cup anemometer than actually generated by the fan. Second, the natural wind could vector add to the fan-generated wind to change the effective wind to the cup anemometer. If sufficiently large, the natural wind could change the direction of the particles through the beam from perpendicular to the beam.

Comparing the correlation functions in Fig. 5 generated by the seeded aerosol, fan generated condition to the correlation functions in Fig. 6 generated by the natural aerosol, natural wind condition (to be discussed later), it is found that the seeded correlation functions are noisier and more ambiguous than natural aerosol correlation functions. This is caused by the large background of small particles in the humidifier generated particles. Note that this shows that multiparticle correlation functions are generally noisier and more ambiguous than single particle correlation functions.

Due to the poor results obtained with seeded aerosol, fan-generated wind, and the absence of rain for several weeks following the previous experiment, the natural aerosol and natural wind condition was attempted. Representative data is presented in Table 4 and representative correlation functions are shown in Fig. 6.

The laser power measured at the sensing volume ranged from 46 mW to 50 mW. The beam separation was approximately 1.15 mm. The cathode voltage of the FMT was 1900 volts.

The data in Table 4 shows excellent agreement between the cup anemometer and the LTV correlator. Other experiments run under similar conditions show this agreement, as long as the natural wind is not too slow and/or as long as the wind direction is not nearly parallel with

Table 4. Comparison of Cup Anemometer Velocity and Average LTV Correlator Velocity for Natural Aerosol and Natural Wind

Cup Anemometer Velocity (m/s)	Average LTV Correlator Velocity (m/s)	Number Data Points in LTV Average Velocity	Propagation Error	Beam Separation ( $\mu$ m)	Sensing Volume Power (mW)
$1.34 \pm 0.5$	$1.17 \pm 0.12$	9	$\pm 0.01$	$1141 \pm 25$	50
$1.32 \pm 0.5$	$1.32 \pm 0.32$	7	$\pm 0.02$	$1141 \pm 25$	50
$0.86 \pm 0.5$	$0.81 \pm 0.11$	5	$\pm 0.01$	$1170 \pm 33$	47
$0.43 \pm 0.5$	$0.53 \pm 0.11$	8	$\pm 0.004$	$1141 \pm 25$	46

the laser beams. Due to the mass of the cup anemometer and digitizing error in the cup anemometer electronics, wind speeds of 1 MPH (0.45 m/s) or less are considered to be too slow. This would tend to suggest that the last entry in Table 4 should not be made. However, a steady wind was blowing at the time. The data indicate that the anemometer reading was a true reading.

Referring to Fig. 6, note that the correlation functions for the natural aerosol with natural wind are relatively noise-free and unambiguous. The correlation functions of Fig. 6b and 6c occurred in the same microprocessor series of 60 experimental runs only one second apart. The laser power at the sensing volume was 43 mW. The cathode voltage of the PMT was 1900 V. The beam separation was  $1141 \pm 25 \mu\text{m}$ . The correlation function of Fig. 6b appears to be a single particle correlation function, while the correlation function of Fig. 6c appears to be multiparticle. Although the total counts for the experimental runs are similar, the multiparticle correlation function, Fig. 6c, has nearly twice the clip counts of the single particle correlation function, Fig. 6b. Further investigation into single particle and multiparticle correlation functions will need to be made to determine if the clip count could indeed be used as an indicator in this connection.

In summary, the best experimental condition for agreement between the cup anemometer and the LTV is, to our satisfaction, natural aerosol and natural wind.

The seeded aerosol and fan generated wind condition suffers from systematic errors in the use of the cup anemometer and in particle generation. The correlation functions obtained are poor compared to those obtained with natural aerosol and natural wind. For the seeded

aerosol, fan generated wind condition to work, a truly single particle generator will be required. Other conventional anemometers should be investigated to determine their suitability in this research.

The standard deviation of the average LTV correlator velocity in Tables 2, 3, and 4 seems large at first until one realizes that the cup anemometer measures wind speed over a time period of 3 seconds whereas the LTV correlator measures wind speed over a time period of several milliseconds or less. Essentially, the cup anemometer measures average wind velocity whereas the LTV correlator measures instantaneous velocity. This suggests that the LTV correlation technique can provide more detailed information, and that the LTV correlator is a better instrument for measuring atmospheric wind than a conventional anemometer.

#### IV. A Method for Measuring Atmospheric Turbulence

Because of atmospheric turbulence, the focussed laser beams may breathe and wander. Therefore, the size of the focussed beams and their separation may change from time to time. Since both laser beams in LTV operation propagate through the same atmosphere, it is expected that the two beams will wander together leaving their beam separation unchanged. This, however, should be tested experimentally. A linear diode array as described below can be triggered at a preset time interval to probe the size and the separation of the laser beams at a time scale comparable to the time-of-flight of a traversing particle in question. This way the effect of atmospheric turbulence on the laser beams at a time scale of a few milliseconds can be determined.

The linear photodiode array, a Reticon Corporation RL-128G array, is composed of a row of silicon photodiodes, each of which is  $15\text{ }\mu\text{m}$  wide by  $26\text{ }\mu\text{m}$  high with  $10\text{ }\mu\text{m}$  between photodiodes. Each photodiode has an associated storage capacitor on which photocurrent is integrated, and a multiplex switch for periodic readout by way of an integrated shift register scanning circuit. Low noise photocurrent pulses are provided by reading out a row of dummy diodes and storage capacitors differentially with the photodiodes to cancel multiplex switching transients.

The differential outputs from the RL-128G linear photodiode array are sent to the Reticon RC301 current amplifier, and clock and counter, circuit board. The current amplifier, composed of discrete elements, provides a pulse output relative to the photocurrent stored by each photodiode. Consideration will be given to replacing the discrete differential amplifier with an integrated differential amplifier to take



advantage of the lower noise characteristics of the integrated differential amplifier. The clock and counter circuit consists of an adjustable frequency clock and a programmable counter from 1 to 4096 counts. The counter controls the start pulse to the photodiode array multiplex readout switch, and thus the interval between start pulses or the total time between line scans, is adjustable. The photodiode to photodiode sampling rate is the clock frequency which is adjustable to a maximum rate of 1 MHz. Due to the possibility of integrated dark current at slower line scanning rates, the maximum real time between start pulses should not exceed 30 milliseconds.

The output pulses from the current amplifier are sent to a peak detector. The peak detector output voltage is sent to an Analog Devices AD7574BD 8 bit microprocessor compatible analog to digital converter for conversion to a digital number. These digital numbers are stored in the microprocessor memory. This process is repeated for as many sweeps as needed, or until the microprocessor memory is filled.

The data stored in the microprocessor will be analyzed to determine beam wander, beam separation changes, and beam diameter changes. Although time did not permit us to interface the diode array with the microprocessor, nor did we perform field tests, the response of the array to laser beams has been observed.

Preliminary results in the lab show the need for the integrated differential amplifier to reduce noise. In the lab, with the short path length, and lack of large scale wind and atmospheric turbulence present in outdoors, the beam separation and diameter was constant, and the beams did not wander. This was accomplished by observing the current amplifier output pulses from the RC301 board on an oscilloscope. We believe that such field experiments using a linear array in this manner,

will produce understanding of the effects of atmospheric turbulence on the performance of LTV for longer ranges.

## V. Conclusions

We have demonstrated that atmospheric wind speeds can indeed be measured with photon bursts scattered from single dust particles. If photon counting electronics and clipped digital correlation are used for signal analysis, an unambiguous speed measurement can be made with a detected signal as low as ten counts under practical conditions, i.e., in the presence of noise. Probability density of photon counts can be measured with the same set-up, and the distribution of atmospheric aerosols may then be investigated. Among other things, such investigation yields agreement in the performance of speed measurements, confirming the theory of single-particle scattering and burst correlation for atmospheric wind speed measurements.

A microprocessor is used to run the LTV measurements automatically. Data from both LTV and a conventional cup anemometer are taken and analyzed by the microprocessor. The whole automated system worked quite satisfactorily, and yielded agreements between the LTV and the cup anemometer. The potential of the LTV lies in its high speed for data acquisition and short measurement time, typically in the order of milliseconds per measurement.

In the field test of this automated LTV system, we have conducted speed measurements with both natural aerosols and with seeding of water droplets from a humidifier. To our satisfaction, we obtained better performance without seeding.

In short, with the research of this project, we have demonstrated beyond doubt the principle of single-particle scattering for remote speed measurements and also demonstrated the practical uses of LTV under realistic field conditions.

### References

1. K. G. Bartlett and C. Y. She, Appl. Optics 15, 1980 (1976).
2. K. G. Bartlett and C. Y. She, Optics Lett. 1, 175 (1977).
3. K. G. Bartlett and C. Y. She, J. Opt. Soc. Am. 69, 455 (1979).
4. C. Y. She, Optica Acta 26, 645 (1979).
5. V. Digiogio and J. G. Lastovka, Phys. Rev. A 4, 2033 (1971).
6. W. M. Fairbank, Jr. and C. Y. She, Optics News, Spring 1979.
7. Hugh D. Young, "Statistical Treatment of Experimental Data", McGraw-Hill, 1962, p. 144, Eq. 13.8.
8. Ibid, p. 140, Eq. 3.9.

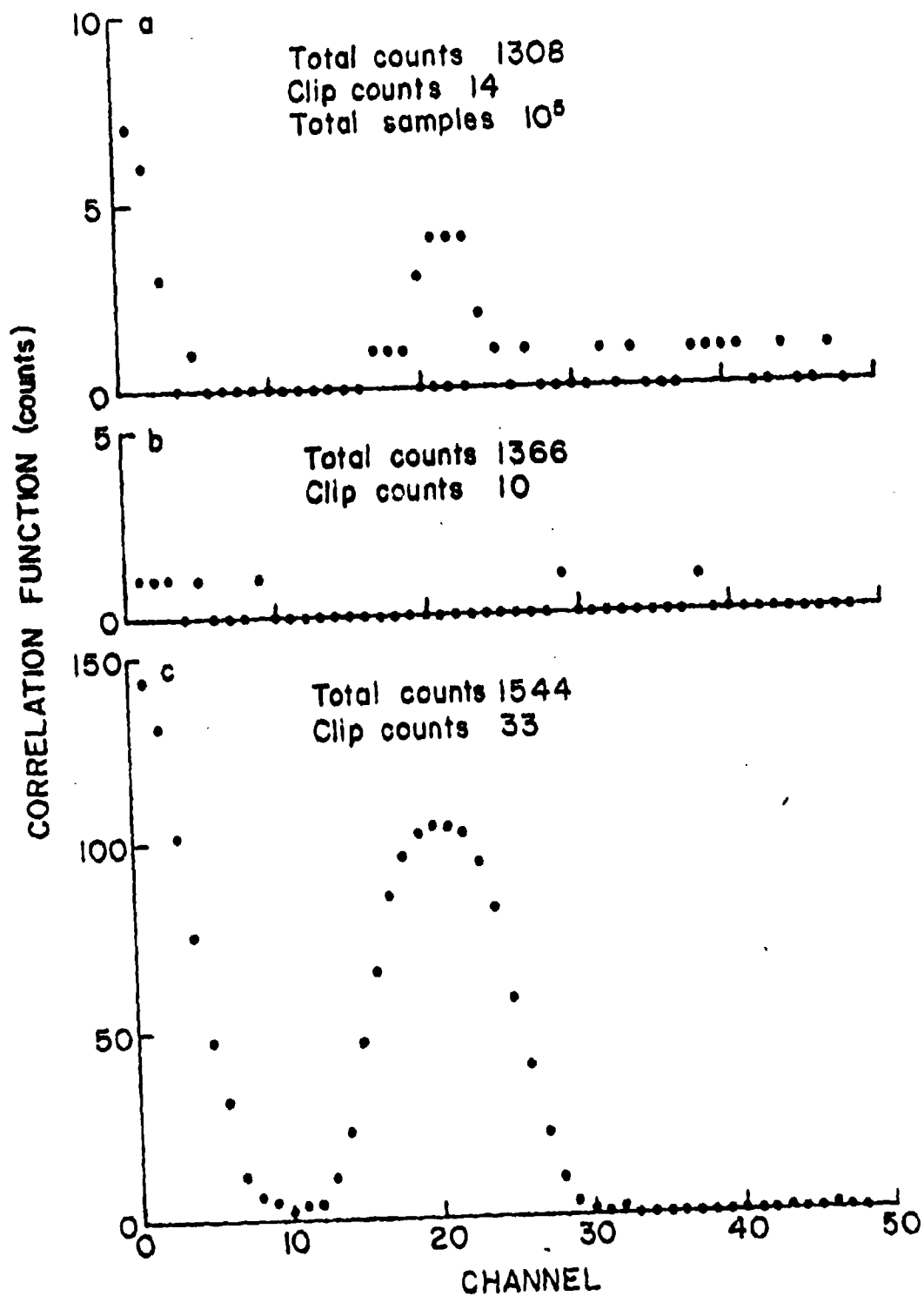


Fig. 1. Three selected correlation functions resulting from natural aerosol indoors.

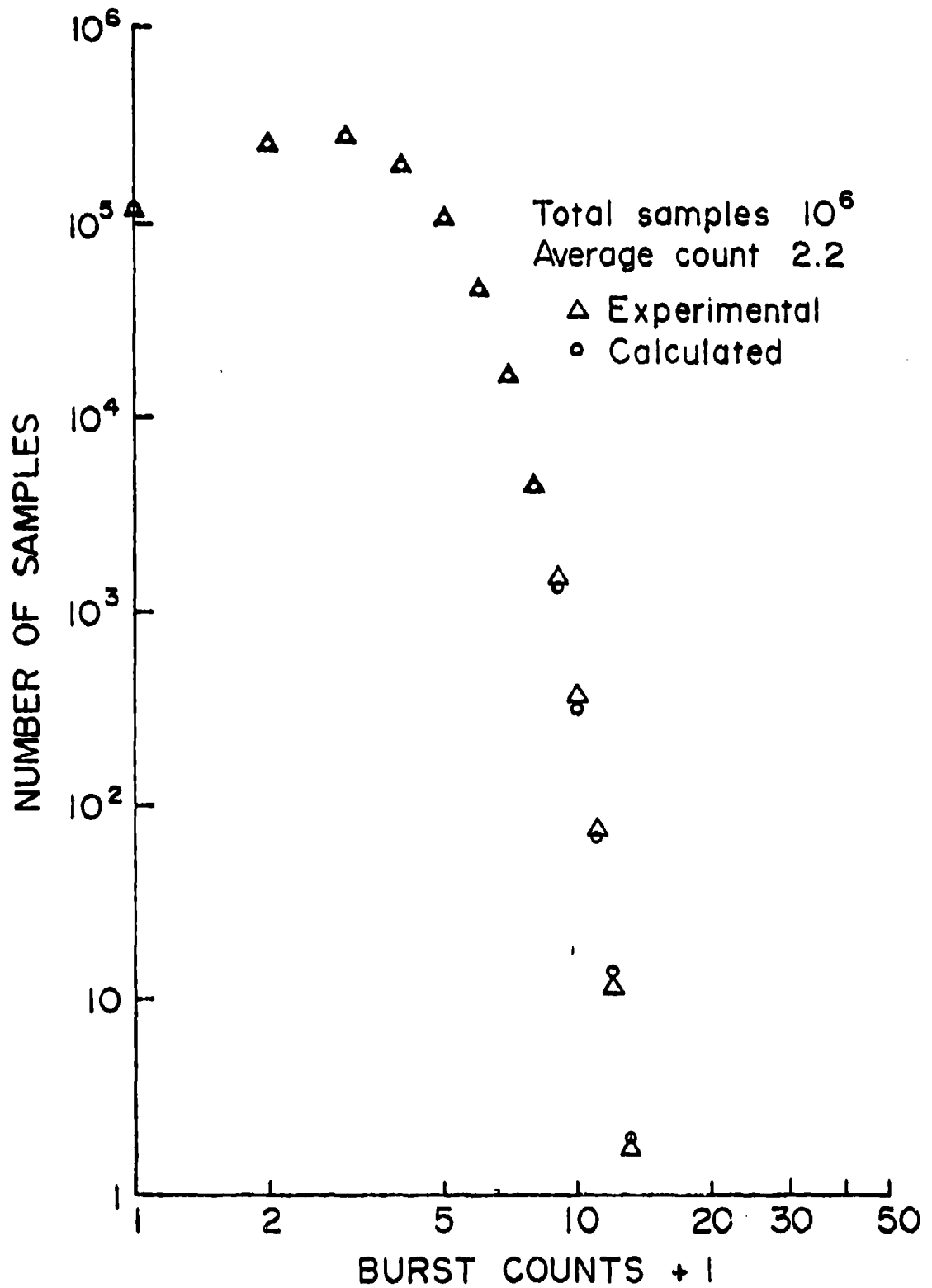


Fig. 2. Probability density of burst counts from a uniformly illuminated target.

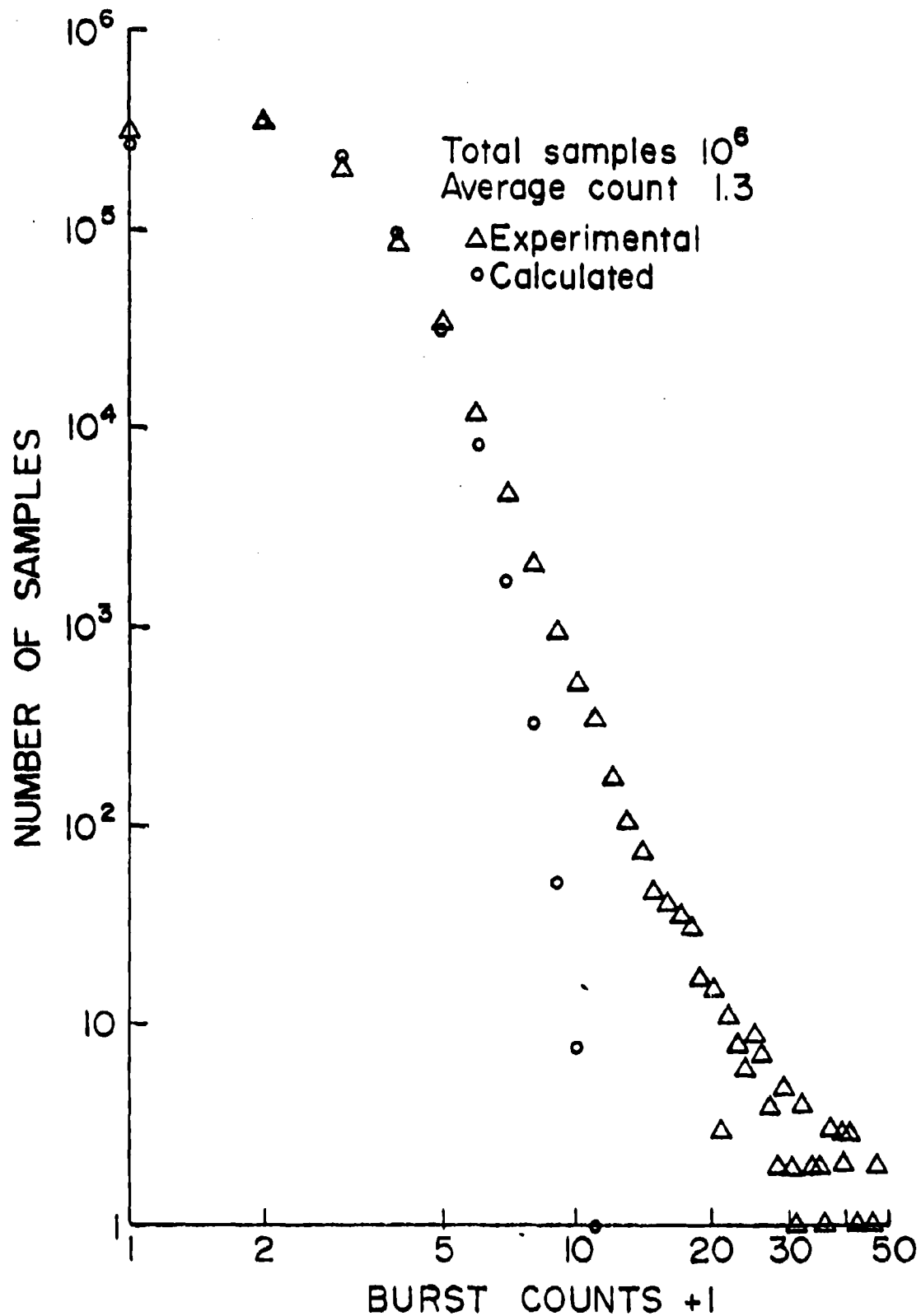


Fig. 3. Probability density of burst counts resulting from indoor aerosol.

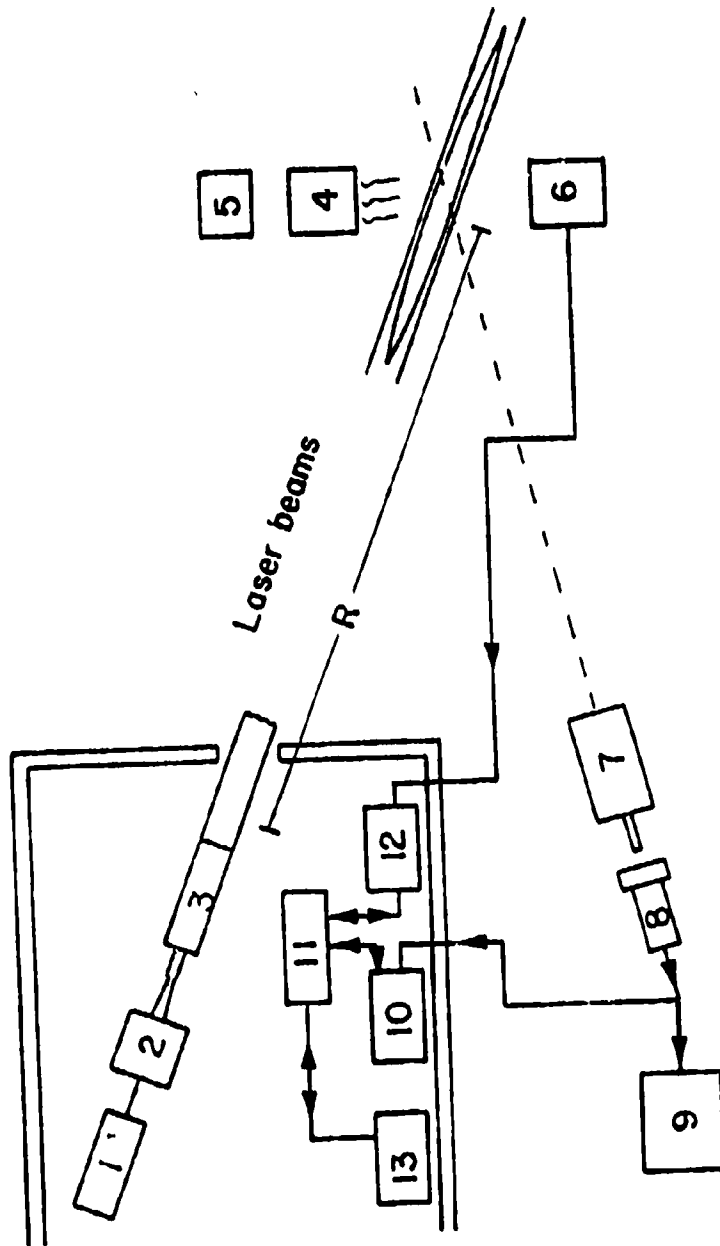


Fig. 4. Experimental arrangement for LTV field measurement. 1. Laser, 2. beam splitter, 3. focussing telescope, 4. fan, 5. particle generator, 6. cup anemometer, 7. receiving telescope, 8. photomultiplier assembly, 9. digital rate meter, 10. digital correlator, 11. micro-processor, 12. anemometer electronics, 13. teletype.



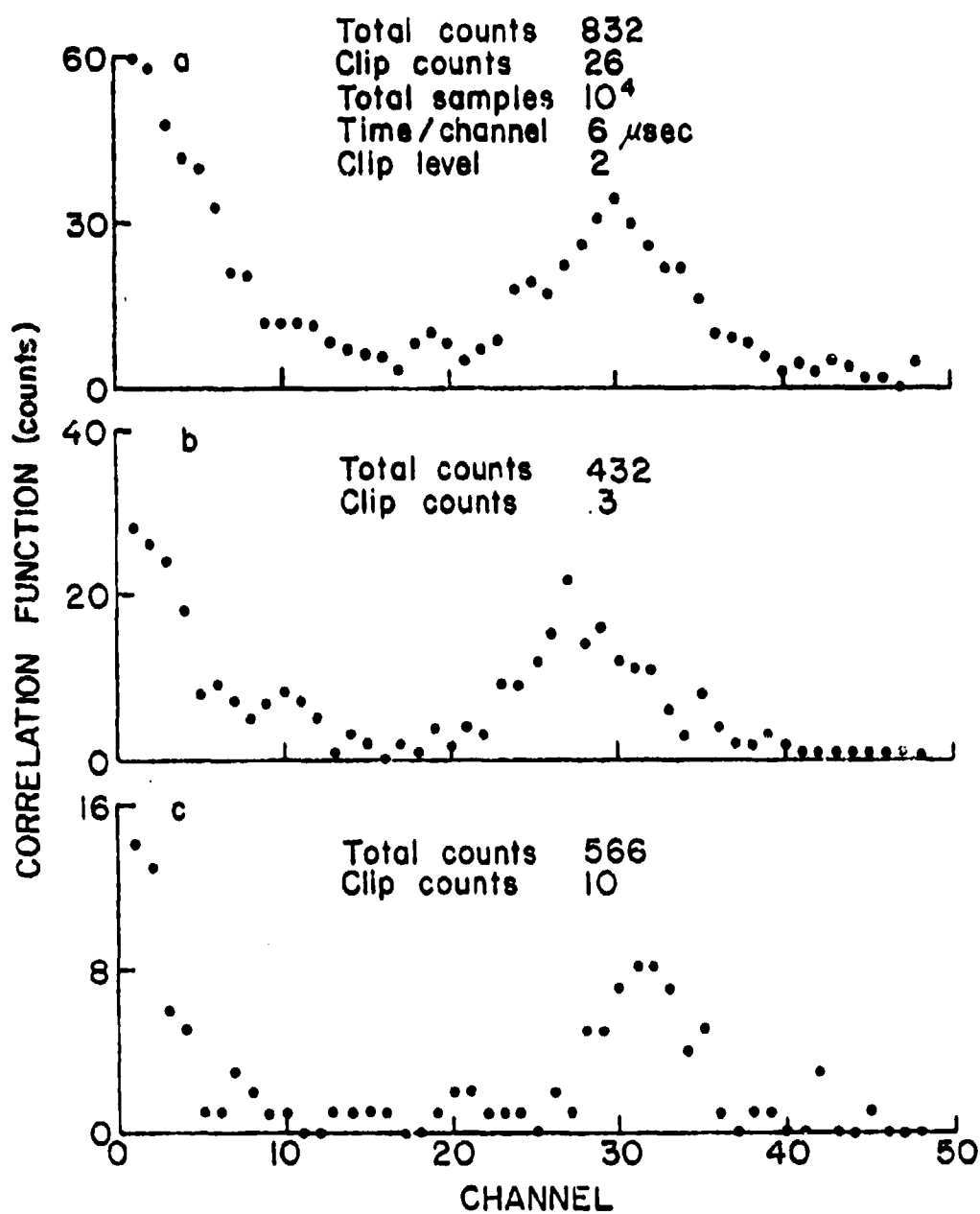


Fig. 5. Typical correlation functions for seeded aerosol and fan generated wind.

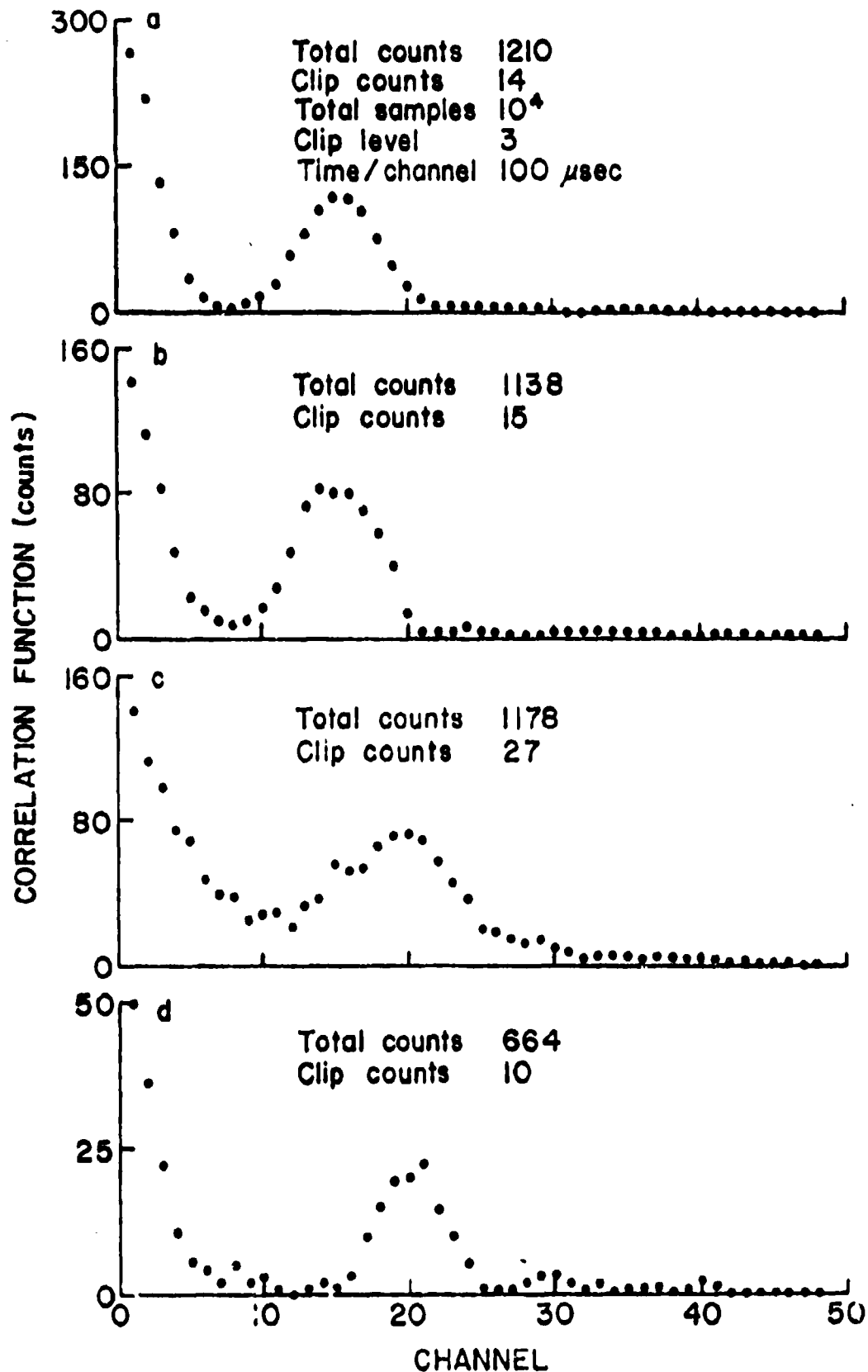


Fig. 6. Typical correlation functions for nature aerosol and natural wind.

## Individual particle scattering and single-burst digital correlation for remote atmospheric wind measurements†

C. Y. SHE

Physics Department, Colorado State University, Fort Collins, Colorado 80523, U.S.A.

(Received 16 January 1979)

**Abstract.** Remote measurements of atmospheric winds by scattering from natural aerosols with a low-power continuous-wave laser have been impressively demonstrated in recent years. Much of the success may be attributed to the use of photon counting in connection with digital correlation techniques and to the realization of the concept which probes individual dust particles. The techniques and requirements for single-burst digital correlation measurements are distinctly different from those of the usual correlation experiment in which the statistical average over an appreciable period of times is taken. These unique differences, as well as the natures of single- and multiple-particle scattering, are discussed. Together with experimental results, this paper presents the unique characteristics of single-burst digital correlation and the methods for applying them to atmospheric wind-speed measurements.

### 1. Introduction

In recent years, there has been a great deal of interest in using the techniques of laser back-scattering, to make single-ended, remote measurements of atmospheric winds in real time, in investigations of the structure and dynamics of the lower atmosphere. Unlike hot-wire or cup anemometers, the laser probe is virtually non-invasive; it can probe very small volumes and reach locations not easily accessible to conventional techniques. Most laser techniques, such as heterodyne laser Doppler velocimetry [1], mono-static lidar [2] or transit-time lidar [3], depend on the presence of many particles within the scattering volume for a signal. Basically, the two lidar techniques make use of back-scattering of laser pulses from large inhomogeneities in the wind-borne particulate densities. Generally, such methods require high-power pulse lasers and are able to reach distances of up to several kilometers; however, they use long measurement times and are limited by poor spatial resolution.

Although it is desirable to use a low-power laser and simple equipment for atmospheric sensing, techniques for transverse wind speed measurements utilizing continuous-wave lasers have been largely neglected. To some extent this is due to predictions which suggested that the dual-beam laser Doppler velocimeter (LDV, the most common transverse technique) was inefficient and not useful at ranges much beyond 2 m for a 1 W argon-ion laser source and not more than 10 m with a multi-watt CO<sub>2</sub> laser. This sort of performance, if true, is not very encouraging.

Before we started our remote sensing programme in summer 1974, LDV systems had long been established as a nearly perturbation-free, speed measurement tools with relatively good spatial resolution in the laboratory. However, to the author's

† This work was supported in part by the Office of Naval Research and monitored by the Optical Radiation Branch of Naval Research Laboratory, Washington, D.C., U.S.A.

knowledge, only one experiment to measure remote atmospheric wind measurements in the field, using a visible wavelength LDV, has been reported in the literature. In that experiment, aerosol scattering in the forward direction [4] was used to provide the velocity signal; it was therefore not a single-ended measurement. By recognizing the fact that the random positions of scatterers in the interference fringe system of an LDV may degrade the velocity signal [5], we designed our system to detect individual particles for wind-speed measurements [6]. This method of single-particle correlation, or single-burst digital correlation, led to a successful atmospheric wind measurement at a range of 60 m using a continuous-wave laser at 5145 Å with only 0.35 W of power. We have also developed performance criteria and proposed the rate of unambiguous speed measurements as the figure of merit for the field experiment. Judging from our experimental results at that time, this figure of merit provided a more meaningful and more accurate evaluation of the system performance than the usual signal-to-noise consideration [5, 7].

More recently, we have developed a new technique of single-particle correlation for measuring the speed of a cross-wind by determining the time of flight of an aerosol particle across two closely spaced, approximately parallel beams [8]. This new laser time-of-flight velocimeter (LTV) suffers less atmospheric effects and requires no coherence between the two beams. As a result, single-ended speed measurements of unseeded atmospheric wind at a range of 100 m using a 0.2 W laser power at a rate of  $1 \text{ s}^{-1}$  have been successfully made. On a different night, the same measurement rate was achieved at a range of 50 m with only 0.015 W of laser power. Very recently, the method of single-particle cross-correlation has also been successfully used to measure the time of flight of individual aerosols in a daytime operation [9].

It is evident that the initial successes in the remote measurement of atmospheric winds by aerosol scattering, using a low-power, continuous-wave laser, are the results of probing individual dust particles and of using photon-counting and single-burst digital correlation (or single-particle correlation) for signal analysis. These concepts have not been discussed in detail in the literature. During the past several years, it has become clear to the author that the differences between single- and multiple-particle scattering are not generally appreciated; neither are the nature and requirements for single-burst correlation clearly or widely understood by scientists and engineers concerned with remote sensing. Therefore, in this paper, the differences between single- and multiple-scattering and the associated signal strength for wind-speed measurements are discussed first. The nature of single-burst digital correlation and the methods for its effective application are then described. Finally, the usefulness of single-particle scattering and single-burst digital correlation, as well as some of their limitations in remote sensing of the atmosphere, are presented.

## 2. Single-particle scattering versus multiple-particle scattering

Perhaps the simplest way to appreciate the differences between single- and multiple-particle scattering is to consider several hypothetical situations of light scattered from dust particles, as depicted in figure 1. Four different combinations of dust particle are shown to traverse a set of interference fringes on the left and two illuminated laser beams on the right. Case A consists of many small particles which scatter an almost constant intensity of light at all times. The small intensity variation detected in this case is the result of fluctuations of Poisson statistics. As can be seen in

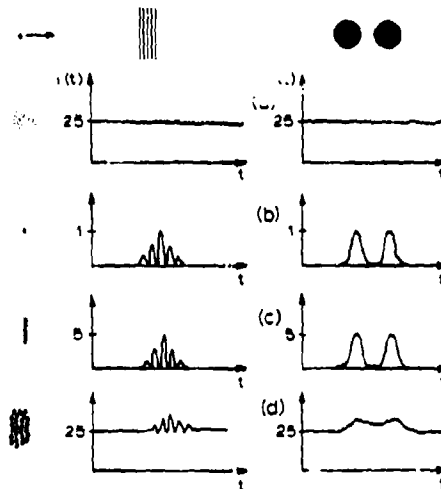


Figure 1. The nature of scattered intensity due to (a) many small particles, (b) one signal particle, (c) five signal particles added constructively and (d) 25 randomly distributed signal particles.

case A, the collective scattering from many small particles yields no useful speed information. If a single particle big enough to yield a burst of light sufficient for a speed signal (we shall call it a signal particle) to traverse the interference fringes and/or the two illuminated beams, the detected scattering intensity maps out the intensity profile of the viewing volume and provides the information necessary for the wind-speed measurement. As shown in case B in figure 1, the scattered intensity is much less than the detected background light of case A, but its temporal variation contains the desired speed information. A physically very unlikely case is case C, in which five signal particles are aligned in parallel to the interference fringes and are traversing the viewing volume together. This is very desirable because the contributions of these particles add constructively to produce a five fold increase in the intensity variation for speed measurements. The small fluctuations in intensities in cases B and C are again statistical. In case D, 25 randomly distributed signal particles are assumed to traverse the scattering volume. The background light is 25 times more intense than that due to one large particle and the variation in intensity which contains the velocity information is much less than 25 times as strong due to destructive interferences resulting from the random positions of these scatterers. As these particles traverse the two illuminated beams, the scattered intensity bursts are much wider, resulting in a partial wash-out of speed information. It is apparent that the signal-to-noise ratio resulting from the 25 big scatterers is no better than that due to a single signal particle of comparable size. In fact, as the number of scatterers continue to increase, the visibility of the interference fringes and illuminated beam profiles, as measured by scattered light, would be washed out and the desired speed information no longer contained in the detected light intensity. Therefore the signal for a speed measurement is best provided by the scattering of a large single particle. Contrary to common beliefs, overabundance of available scatterers can in fact hinder

the remote velocity measurements. This is especially true for atmospheric measurements because the instantaneous wind speed changes from one instant to the next, and time-averaging does not enhance the desired speed signal.

One wonders, perhaps, whether a single aerosol particle could in fact scatter enough light for speed measurements. A simple calculation would suggest that a particle a few micrometers in size will scatter enough photons to yield an unambiguous digital correlation for wind-speed measurements. For simplicity, let us consider a particle  $2\text{ }\mu\text{m}$  in diameter which back-scatters light from a  $0.1\text{ W}$ ,  $0.5\text{ cm}$  diameter laser beam at a distance of  $20\text{ m}$  from the detector. The back-scattering differential cross-section [10] is approximately  $0.2r^2$  where  $r$  is the radius of the particle. Since the laser intensity is  $0.5\text{ W/cm}^2$ , the differential back-scattered power would be  $(0.5)(0.2)(1 \times 10^{-4})^2 = 1.0 \times 10^{-9}\text{ W/sr}$ . With a  $20\text{ cm}$  diameter receiving telescope, the detection solid angle is  $7.85 \times 10^{-5}\text{ sr}$ . For a laser at  $5145\text{ \AA}$  and a photomultiplier tube with 20 per cent quantum efficiency, the detected photon rate is calculated to be  $4 \times 10^4$  counts per second. If the particle's transverse velocity is  $100\text{ cm/s}$ , it stays in the  $0.5\text{ cm}$  beam for  $5\text{ ms}$ , giving rise to a total detection of 200 photons. This is quite adequate for obtaining a single-burst digital correlation to determine wind speed. In practice, more than  $0.1\text{ W}$  of power could be used to enhance the desired single-particle signal for measurements at longer ranges.

### 3. Properties of single-burst digital correlation

When the signal is weak, the process of correlation can be used to discriminate against noise, so enhancing the detectable signal. Because noise fluctuations are uncorrelated, averaging over a longer period of time usually helps a weak signal to accumulate and grow. However, for non-stationary processes, such as the motion of particulate matter in the atmosphere with the instantaneous velocity changing from time to time, the usual technique of time integration does not help the enhancement of the desired correlation signal. As described earlier, under such conditions it is best to take advantage of individual particle scattering and complete the correlation function from the photon bursts of a single event, giving rise to what might be called a single-burst digital correlation. An example of such a computation is shown in figure 2. Here, the scattered signal photon counts are the result of a single dust

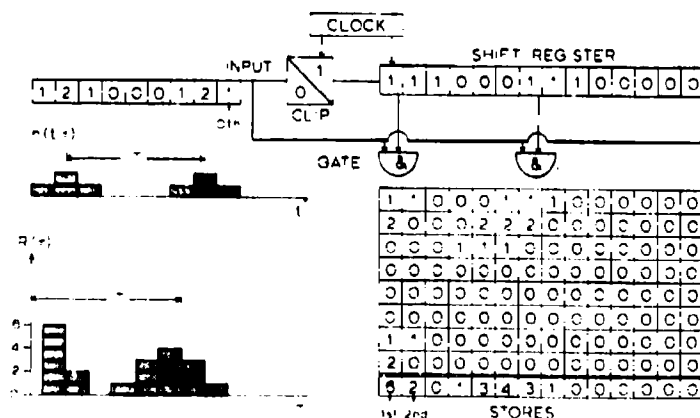


Figure 2. An example of the operation of single-clipped digital correlation.

particle traversing two beams of light. The signal shown in this example is very weak, yielding only one or two counts in a sample time. If the stray light noise can be made negligible, the single-burst digital correlation is seen to give a maximum of six counts over the uncorrelated background; the correlation function is thus a definite improvement over the original signal. In practice, there is noise in addition to the desired signal. If the signal strength is comparable with or greater than that of noise, the technique of clipping can be used to advantage. The clipping level is then set above the average noise background and the survival counts should then reflect mostly the behaviour of the desired signal.

Some examples of single-burst correlation functions are shown in figures 3 and 4. These are correlation functions obtained from field measurements of atmospheric winds at a range of 20 m. Figures 3 and 4 correspond to LDV and LTV arrangements

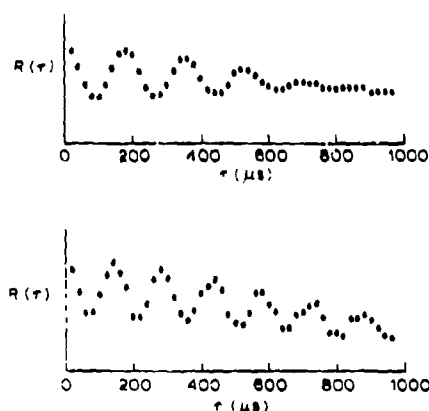


Figure 3. Two LDV correlation functions obtained from a field experiment at a range of 20 m with 0.2 W laser power, and a correlator setting of 20  $\mu$ s per channel and a clipping level of 8.

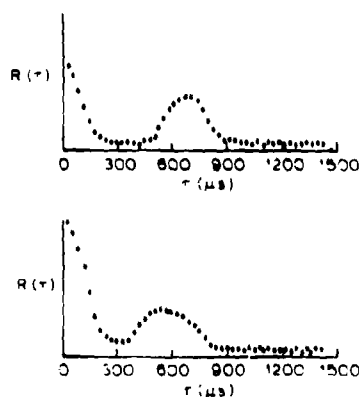


Figure 4. Two LTV correlation functions obtained from a field experiment at a range of 20 m with 0.03 W laser power, and a correlator setting of 30  $\mu$ s per channel and a clipping level of 5.

respectively. These single-burst correlation functions were obtained by turning the correlator on and off. An oscilloscope was used to monitor and display the measured correlation functions. Immediately after the correlator was turned on, no correlated signal was observed on the oscilloscope for, typically, a fraction of a second (the exact time depends on laser power and measurement range). As a signal particle, i.e. a particle big enough to give unambiguous speed information, moved across the viewing volume, a correlation function was suddenly recorded in about 1 ms, depending on the speed of the moving particle. The correlator was then turned off and reset for the next measurement.

The fact that the field data such as those shown in figures 3 and 4 correspond to a burst of signal resulting from, primarily, a single signal particle traversing the viewing volume, has been demonstrated previously [6, 8] by noting that accumulation of the signals from several consecutive particles had led to a washing-out of the wind-speed data. To make this point more clear, the detected scattering intensities and the corresponding correlation functions due to a single particle and two closely spaced particles traversing a set of interference fringes are compared in figure 5.

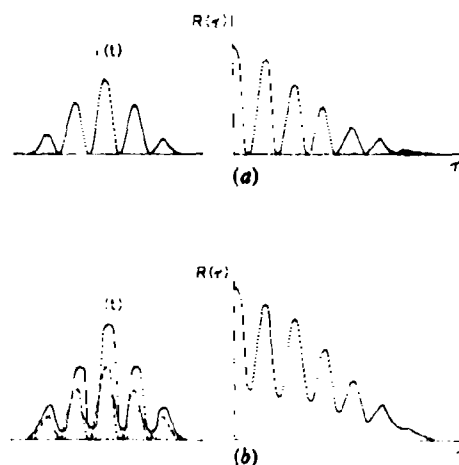


Figure 5. A comparison of the correlation functions resulting from the scattering of (a) single particle and (b) two particles in an LDV arrangement.

When a single particle traverses the intensity fringes, the scattered intensity  $i(t)$  shows maximal visibility and the minima in the correlation function occur at the same count level. When two out-of-step particles traverse the fringes at the same time, the scattered intensity shows much less visibility and the count level of the correlation minima decreases as the correlation time increases. By comparing the prediction of figure 5 to the LDV field data of figure 3, it is apparent that the top correlation spectrum in figure 3 is due to a single dust particle, while the bottom spectrum may result from two particles together. Figure 6 shows the prediction of the scattered intensities and correlation functions resulting from one and two particles traversing two illuminated beams. As expected, the minimum between the two humps in the correlation function dips to the background level when a single particle traverses the two beams. However, when there are two particles together,



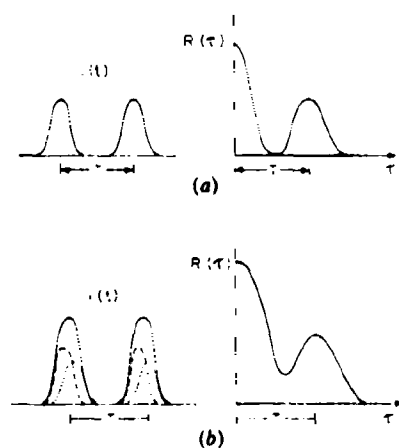


Figure 6. A comparison of the correlation functions resulting from the scattering of (a) a single particle and (b) two particles in an LTV arrangement.

not only is the minimum between humps somewhat higher, but also the width of the humps in the correlation function broadens. Again, the predictions depicted in figure 6 agree with the observed LTV field data shown in figure 4.

#### 4. Methods for obtaining a single-burst correlation function

To further illustrate the application of single-burst digital correlation for wind-speed measurements and to explore the nature of signal counts associated with this type of experiment, an LTV system was set up to measure simulated winds in the laboratory. Two laser beams at 5145 Å are crossed to produce a set of intensity fringes with a fringe spacing of approximately 200  $\mu\text{m}$ , and the natural dust particles in the room were blown across them by a fan. To minimize the stray light, several baffles were placed between the scattering volume and the photodetector. The correlator was turned on until a single-burst correlation function was observed on the monitoring oscilloscope, when the correlator was reset for the next experiment. Table 1 gives the results of three consecutive speed measurements. The first four channels, 00, 01, 02 and 03, are counters giving respectively the total signal counts, the total clipped counts, zero, and the total number of samples taken during the experiment. The 02 channel gives the signal counts of another input; it therefore registers zero for autocorrelation experiments. Channels 04 to 51 give the measured single-clipped correlation counts for 48 delay channels [11]. Using these counts, the correlation functions for the wind-speed measurements are plotted in figure 7. It is evident from these graphs that particles of different sizes can be used for wind-speed measurements. Since the dust particles are blown by an electric fan, the wind speed in question is expected to be nearly constant. This is indeed the case, as shown in figure 7. The strength (or counts) of the measured correlation depends on the size of the scattering particle. The correlation shown in figure 7(c) has 20 times as many counts as compared to that shown in figure 7(a). The measured speed shown in figure 7(c) is slightly slower, indicating perhaps that the larger particle cannot faithfully follow the flow.

Table 1. Correlation counts for three consecutive measurements.

Channel marker		Correlation counts				
(a)	00	5185	6	0	142804	36
	05	27	20	11	7	2
	10	4	14	24	28	22
	15	16	11	8	3	0
	20	3	8	11	13	9
	25	6	1	0	0	1
	30	2	3	5	5	7
	35	7	7	4	1	1
	40	1	2	1	2	5
	45	6	6	4	2	2
	50	1	1			
(b)	00	7149	24	0	197913	114
	05	91	64	41	23	30
	10	46	66	95	114	106
	15	92	64	40	24	21
	20	31	56	80	79	78
	25	76	57	40	23	14
	30	19	35	47	57	66
	35	54	38	30	14	10
	40	9	17	27	31	44
	45	33	32	19	12	11
	50	3	8			
(c)	00	10114	49	0	270418	766
	05	670	557	480	467	506
	10	583	698	753	743	639
	15	516	426	361	375	443
	20	516	610	594	527	429
	25	316	261	238	285	363
	30	408	422	399	323	250
	35	160	159	160	202	244
	40	253	243	220	158	113
	45	87	101	121	125	158
	50	153	141			

It is interesting to note that the average count per channel (or per sample time) for the data given in table 1 is about the same, 0.036, 0.036 and 0.037 respectively for the three consecutive measurements, although the correlation strengths are quite different for the three runs. Because the average count per sample time was much less than the clipping level (set at 4), most of the random background fluctuations due to scattering from small particles or reflections from optical components were clipped out. The fact that the correlation levels vary by a factor of 20 without affecting the average count per channel indicates that the particle whose speed is being measured traverses the viewing volume only for a short time. This indeed agrees with observation, and with the expectation of single-burst correlation. The data shown in figure 7 (a) and table 1 (a) have only six clipped counts in a total of 142 804 samples, which means that the useful signal counts exceeded the clipping level of 4 less than six times in over 140 000 samples. Of the six samples, one or two might possibly

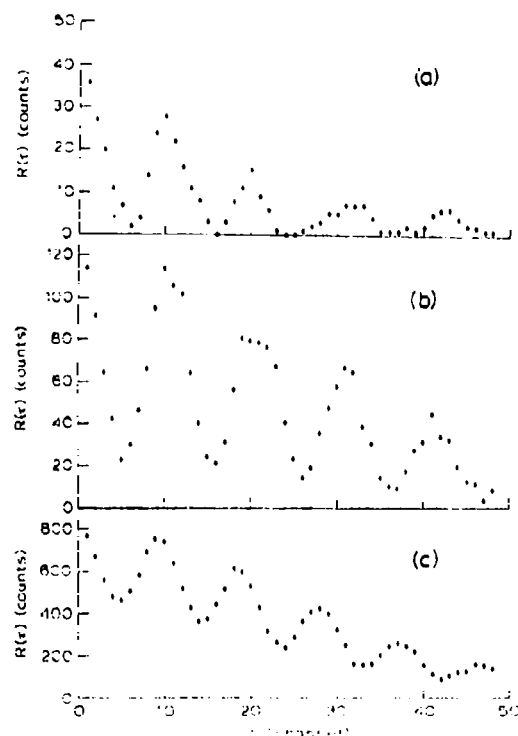


Figure 7. Three consecutive, single-burst digital correlation functions resulting from different-sized signal particles traversing a set of intensity fringes in an LIDV set-up with 0.1 W laser power, and a correlator setting of 50  $\mu\text{s}$  per channel and a clipping level of 4.

result from noise fluctuations that occasionally exceed the clipping level, yet this is enough to produce a distinct correlation function for speed measurement, as shown in figure 7(a). Although the last two oscillations in figure 7(a) may have been distorted by the presence of random noise, the first three provided accurate readings for wind-speed determination. The sensitivity of the method of single-burst correlation for speed measurements is evidently excellent, as expected.

An alternative method may be used to carry out these measurements. The correlator could be turned on for a preset time interval which is shorter than the particle's time of transit across the intensity fringes. If a particle happens to traverse the viewing volume during this time, an unambiguous wind-speed signal is recorded. However, during many tries there will be no signal particle traversing the scattering volume, so no useful correlation function can be recorded. The frequency of successful speed measurements thus depends on the availability of signal particles. In order to determine the preset measurement time, the experimental conditions need to be examined. The fringe spacing of the experimental set-up used previously was approximately 200  $\mu\text{m}$  and the transverse dimension of the viewing volume was about 0.4 cm. Since the time per sample of the correlator was set at 50  $\mu\text{s}$  per channel, the measured wind speed from data shown in figure 7 was approximately 40 cm s<sup>-1</sup>.

The time a particle took to cross the viewing volume was calculated to be  $10^{-2}$  s or 200 samples. If the measurement time was preset at 0.05 s, or a total of 1000 samples, it was found that on average one out of five tries yielded adequate correlation functions from which the desired wind speed could be determined. If the measurement time was set for 100 samples while keeping other experimental conditions unchanged, the average frequency for successful measurements became approximately 1 in 50, as expected. Although the measurement time,  $5 \times 10^{-3}$  s, is less than the beam crossing time, the particle during the measurement could have traversed several fringes to permit a successful determination of the desired wind speed. When signal particles are available, the measurement time needed to carry out single-burst correlation is indeed very small; it took only 5 ms for the above example.

When operating a digital correlator with such a short measurement time (e.g. 100 samples), as required in single-burst digital correlation, certain precautions should be taken. Firstly, the shift register in the correlator should be reset to zero before an experiment, otherwise the digits left over in the shift register from an earlier measurement will affect the result of the new one. The shift register does not reset automatically in some commercial correlators, in which case a null experiment must be made to clear out the digits in the shift register between measurements. Secondly, if the input signal level is consistently higher than the clipping level set, a monotonically decreasing correlation function will result. By practising the operation of single-burst digital correlation, one quickly learns how to cope with the situation and to prevent these mishaps from occurring. These precautions are not necessary in a normal correlation experiment [12] when the statistical average is taken over a much longer time.

## 5. Discussion

The techniques of single-burst digital correlation (or single-particle correlation) have been used effectively to measure atmospheric wind speeds [6, 8, 9]. The sensitivity achievable with single-burst correlation approaches the level of a few detected photons. As a result, instantaneous atmospheric wind speeds could easily be measured at a range of up to 100 m at this point by using a low-power, continuous-wave laser (about 0.2 W). The extension of the proven techniques to measure the instantaneous wind velocity vector should be straightforward.

The fact that the methods of single-burst digital correlation depend on the arrival of individual signal particles has been proved experimentally and theoretically. An unambiguous rate for wind-speed measurements has been shown to agree with the concentration of available signal particles [6, 8], and the measured power and range dependences of the measurement rate has been shown to agree with the measured distribution of signal particles [13] under the same atmospheric conditions. In this paper, the difference between individual- (or single-) particle scattering and multiple-particle scattering has been discussed. Experiments in the laboratory have yielded correlation functions that not only agree with the shape of the theoretically predicted single-burst correlation functions, but also produce the expected behaviour and sensitivity of signal and noise for a single scattering event. Direct measurements with preset measurement times as short as 5 ms, which is shorter than the transit time of the signal particle in question, have proved beyond doubt that the measured single-burst correlation is indeed the result of a single scattering event and that no time integration is involved in these experiments.

As the range of measurement increases, the scattered power from a signal particle will of course decrease, and more laser power must then be used. Our theoretical analysis and experimental results have suggested that only 6 W of laser power is needed if single-ended wind-speed measurements at one per second at a range of 1 km is desired [8, 13]. In addition to power limitations, atmospheric turbulence, which prevents the laser beam from focusing, also imposes some limitations on the ultimate success of the single-burst correlation technique. As the following discussion shows, the turbulence effects are of concern only at ranges greater than 1000 m.

Most of the turbulent effects can be described by two range-dependent limiting diameters,  $r_0^{LT}$  for long-term (refractive) effects and  $r_0^{ST}$  for short-term (diffractive) effects [14, 15]. A laser beam therefore wanders through an angle of  $\lambda/r_0^{LT}$  on longer 'exposures' due to large-scale inhomogeneities and spreads (or breathes) through an angle of  $\lambda/r_0^{ST}$  on short-term 'exposures' due to small-scale inhomogeneities. The magnitudes of  $r_0$  ( $r_0^{LT}$  and  $r_0^{ST}$ ) depend on the range,  $R$ , and the wavelength,  $\lambda$ . For a Kolmogorov structure of turbulence with a given refractive-index structure parameter,  $C_n^2$ , the limiting diameter  $r_0$  scales with range and wavelength as

$$\lambda^{-2} R r_0^{5/3} = \text{constant} \quad \text{or} \quad r_0 \propto \lambda^{6/5} R^{-3/5}.$$

At a range of 15 km, Ochs and Lawrence [16] have measured the daytime beam wander and beam spread of a He-Ne laser ( $\lambda = 0.6328 \mu\text{m}$ ) to be 400 and 100  $\mu\text{rad}$  respectively. This means that the short-term limiting diameter at a range of 15 km for a He-Ne laser is  $r_0^{ST} = 0.6328/100 = 6.3 \text{ mm}$ . Scaled to the ranges and argon-ion laser wavelength ( $\lambda = 0.514 \mu\text{m}$ ), the turbulence parameters as a function of range are summarized in table 2, in which  $d^{ST}$  is the diffracted spot diameter due to atmospheric turbulence and  $d$  is the diffraction-limited spot size for a 10 cm telescope without atmospheric effects. Since we are measuring the speed of a single dust particle, the measurement time is typically less than 1 ms in the field; the long-term turbulence effects reported in the literature, such as beam wander, cannot even take place before the measurement is over. Assuming that the short-term turbulence is of importance, the spot diameter can still be focused to 2 cm at 1 km, which is adequate for both LDV and LTV measurements. Measurements up to 2 km are still possible, although the performance would not be as good as predicted. It is not clear what types of short-term effect are most significant for measurements within 1 ms. If, for typical paths and wind velocities, the temporal-frequency spectra [17] are below 500 Hz [18], the atmosphere, at a time-scale less than 1 ms, could be considered as frozen blobs of refractive-index inhomogeneities. In this case, the only effect of turbulence that would degrade the performance of single-particle LDV and LTV is the diffraction effects by inhomogeneous refractive indices. The effective  $d^{ST}$

Table 2. The diameters of focused beam size under atmospheric turbulence.

$R$	$r_0^{ST}$	$d^{ST}$	$d$
100 m	10.5 cm	0.54 mm	0.54 mm
500 m	4.1 cm	6.59 mm	2.70 mm
1000 m	2.6 cm	2.03 cm	5.40 cm
2000 m	1.7 cm	6.35 cm	1.08 cm

would probably be smaller than those listed in table 2. Due to the saturation effect of atmospheric turbulence [19], the temporal and spatial fluctuations at long ranges should in fact be slower and weaker than are predicted without saturation. The performance should obviously be further improved if a near-infra-red laser is used.

To gain some idea of the validity of the above analysis of atmospheric turbulence, we look for interference intensity fringes at a range of 1 km. We have observed high-contrast interference fringes produced by unfocused beams, covering an area several centimeters in diameter, which were stable enough for LDV measurements. Likewise, in order to establish the accuracy of the 'turbulent' spot diameter  $d^{\text{AT}}$  discussed above, we carried out a field experiment one afternoon to observe the spot sizes of an LTV set-up. At a range of 450 m, the diameter of our focused laser spots was between 6 and 7 mm, in agreement with the data given in table 2. The two laser spots of our LTV system wander at a slow rate (several seconds) over a small distance (less than 0.5 cm). Due to the fact that they are propagated through an identical atmosphere, the two spots wander, not independently, but in unison. It appears that atmospheric turbulence should not impose limitations on the single-burst correlation techniques within a range of 1 km.

In summary, the characteristics of single-burst digital correlation have been presented and the methods for obtaining the associated correlation functions have been discussed and demonstrated experimentally. All the theoretical predictions and expectations have been confirmed by our experimental results. Considerations of some limiting factors, including the effect of atmospheric turbulence, and investigations of previous experimental results, led to the conclusion that our single-particle LDV and LTV are not only the result of individual particle scattering but are also capable of measuring atmospheric wind speeds up to a range of 1 km using a low-power, continuous-wave laser.

In den letzten Jahren gab es eindrucksvolle Demonstrationen von Fernmessungen an atmosphärischen Winden durch Streuung an natürlichen Aerosolen mit leistungsschwachen Dauerstrichlasern. Viele dieser Erfolge können der Anwendung von Photonen-zählern in Verbindung mit digitalen Korrelationsverfahren zugeordnet werden, sowie der Verwirklichung des Konzepts zum Nachweis einzelner Staubpartikel. Technik und Voraussetzungen der digitalen Photonenkorrelation sind grundsätzlich verschieden vom üblichen Korrelationsverfahren, bei dem statistische Mittel über erhebliche Zeitintervalle bestimmt werden. Diese eindeutigen Unterschiede als auch die Natur der Einzelpartikelstreuung und der Mehrpartikelstreuung werden diskutiert. Neben experimentellen Ergebnissen präsentiert die vorliegende Arbeit die einzigartigen Charakteristika der Photonenkorrelation sowie deren Anwendung zur Messung atmosphärischer Windgeschwindigkeiten.

## References

- [1] LAWRENCE, T. R., WILSON, D. J., CRAVEN, C. E., JONES, I. P., HUFFAKER, R. M., and THOMSON, J. A. L., 1972, *Rev. scient. Instrum.*, **43**, 572.
- [2] ELORANTA, E. W., KING, J. M., and WEINMAN, J. A., 1975, *J. appl. Met.*, **14**, 1485.
- [3] ARMSTRONG, R. L., MARON, J. B., and BARRER, T., 1976, *Appl. Optics*, **15**, 2891.
- [4] BOUBKE, P. J., and BROWN, C. G., 1971, *Optics Technol.*, **3**, 23.
- [5] SHE, C. Y., and WALL, L. S., 1975, *J. opt. Soc. Am.*, **65**, 69.
- [6] BARTLETT, K. G., and SHE, C. Y., 1976, *Appl. Optics*, **15**, 1980.

- [7] FARMER, W. M., and BRAYTON, D. B., 1971, *Appl. Optics*, **10**, 2319.
- [8] BARTLETT, K. G., and SHE, C. Y., 1977, *Optics Lett.*, **1**, 175.
- [9] LADINO, L., SKOV JENSEN, A., FOO, C., and ANDERSEN, H., 1978, *Appl. Optics*, **17**, 1486.
- [10] HUGHES, J., and PIKE, E. R., 1973, *Appl. Optics*, **12**, 597.
- [11] JAKEMAN, E., and PIKE, E. R., 1969, *J. Phys.*, **A**, **2**, 411.
- [12] SHE, C. Y., and LUCERO, J., 1973, *Optics Commun.*, **9**, 300.
- [13] BARTLETT, K. G., and SHE, C. Y., 1979, *J. opt. Soc. Am.* (in the press).
- [14] FRIED, D. L., 1966, *J. opt. Soc. Am.*, **56**, 1372.
- [15] YURA, H. T., 1973, *J. opt. Soc. Am.*, **63**, 567.
- [16] OCHS, G. R., and LAWRENCE, R. S., 1969, ESSA Technical Report ERL 106-WPL6.
- [17] CLIFFORD, S. F., 1971, *J. opt. Soc. Am.*, **61**, 1285.
- [18] LAWRENCE, R. S., 1972, *Sixth Instrumentation Symposium*, Albuquerque, New Mexico.
- [19] CLIFFORD, S. F., OCHS, G. R., and LAWRENCE, R. S., 1974, *J. opt. Soc. Am.*, **64**, 148.